AVAZ inversion for fracture orientation and intensity: a physical modeling study

Faranak Mahmoudian and Gary F. Margrave

ABSTRACT

We present a pre-stack amplitude inversion of P-wave data for fracture orientation and intensity. We test the method on multi-azimuth multi-offset physical model reflection data acquired over a simulated fractured medium. Our simulated fractured medium is composed of phenolic material with controlled symmetry planes, and its elastic properties have already been determined using traveltime analysis. This experimental model represents a HTI layer. We follow Jenner (2002) for amplitude inversion of small incident angle data to extract the fracture orientation (direction of isotropic plane of the medium), and are able estimate the fracture orientation quite accurate. By knowing the fracture orientation, we have modified the linear PP reflection coefficient equation given by Rüger (2001) to invert for anisotropy parameters $(\epsilon^{(V)}, \delta^{(V)}, \gamma)$. We incorporated some constraints on the vertical velocities and density in the inversion process. Large-offset data are required for the azimuthal amplitude inversion of the simulated fractured layer, as the material shows only slight azimuthal amplitude variations. The results for all three anisotropy parameters from AVAZ inversion compare very favorably to those obtained previously by a traveltime inversion. This result makes it possible to compute the shear-wave splitting parameter, γ, historically determined from shear-wave data, which is directly related to fracture intensity, from a quantitative analysis of the PP reflected data.

INTRODUCTION

The ultimate goal of using AVO in fracture-detection studies is to invert the seismic data for fracture orientation (stike) and the magnitude of fracture intensity. Open natural fractures may hold fluid and can provide pathways for hydrocarbon flow. Detailed information about fracture intensity and orientation can help optimize the drilling at sweet spots (Zheng, 2006). Fracture orientation is defined as the dominant direction of fracture faces. Fracture intensity is the product of the number of fractures per unit volume and their mean cubed diameter (Nelson, 2001). Depending on the stress regime that causes fracturing, the fracture orientation (however random) has a dominant direction confirmed by geological field measurements (Nelson, 2001).

The effect of natural fractures, when seismic waves propagating through them, can be well described by a medium with transverse isotropy (TI). Particularly, aligned vertical penny-shaped fractures embedded in an isotropic horizontal background can be described by a medium with horizontal transverse isotropy (HTI) symmetry (e.g., Thomson, 1986; Tsvankin, 2001).

Assuming fractures can be described by an HTI medium, the azimuthal dependence of P- and S-wave stacking velocities and reflection amplitudes has been used to extract the information about the fracture intensity and orientation. The shear-wave splitting phenomena due to fractures, has been historically used to detect fracture orientation (the direction

of the fast S-wave). The shear-wave splitting factor, γ, directly related to fracture intensity, has also been determined from an analysis of time delays of split shear waves (Crampin, 1981). Using P-wave NMO velocity variation with azimuth (VVAZ), fracture orientation is considered to be in the direction of the fast P-wave. Some indicator of fracture intensity results from estimating the Thomsen δ parameter (e.g., Tsvankin, 2001; Grechka et al., 1999). Zheng and Wang (2005) used a target-oriented VVAZ approach, in which the differential residual NMO travel times between the top and the base of a fractured layer is used to invert for fracture orientation and Thomsen δ parameter. Quantitative amplitude analysis is also used for fracture detection, as in amplitude variation with the angle and azimuth (AVAZ) method. Jenner (2002) reformulated the Rüger (2001) equation for P-wave reflection coefficient from a boundary of two HTI layer, to directly invert for fracture orientation and the anisotropic gradient (a combination of δ and γ parameters) from azimuthal amplitude data.

We present a derivation for an AVAZ inversion for fracture orientation, similar to that used by Jenner (2002), on physically modeled data acquired over a simulated fractured medium. We initially characterized this simulated fractured layer as a HTI layer with known symmetry directions, using traveltime analysis on transmission data and estimated all its elastic properties including the Rüger's parameters $(\epsilon^{(V)}, \delta^{(V)}, \gamma)$. The result for the fracture orientation is quite accurate. We also propose a pre-stack amplitude inversion of large-offset P-wave data, based on Rüger's equation, to to invert for $(\epsilon^{(V)}, \delta^{(V)}, \gamma)$, which γ is directly related to fracture density. We achieve successful inversion results by applying some constraints on vertical P- and S-wave velocity, and density.

THEORY

Fracture density

A plane-wave approximation for the PP reflection coefficient at a boundary between two HTI media with the same orientation of the symmetry axis was developed by Rüger (2001). Rüger's equation for the HTI media with the symmetry axis along ϕ_0 azimuth is

$$\begin{aligned} R_{PP}^{HTI}(\theta,\phi) \cong & \frac{1}{2}\frac{\Delta Z}{\bar{Z}} \\ & + \frac{1}{2}\left\{\frac{\Delta\alpha}{\bar{\alpha}} - \left(\frac{2\bar{\beta}}{\bar{\alpha}}\right)^2\frac{\Delta G}{\bar{G}} + \left[\Delta\delta^{(V)} + 2\left(\frac{2\bar{\beta}}{\bar{\alpha}}\right)^2\Delta\gamma\right]\cos^2(\phi-\phi_0)\right\}\sin^2\theta \\ & + \frac{1}{2}\left\{\frac{\Delta\alpha}{\bar{\alpha}} + \Delta\epsilon^{(V)}\cos^4(\phi-\phi_0) + \Delta\delta^{(V)}\sin^2(\phi-\phi_0)\cos^2(\phi-\phi_0)\right\}\sin^2\theta\tan^2\theta. \end{aligned} \tag{1}$$

where θ is the incident angle, ϕ is the source-receiver azimuth, α is the vertical P-wave velocity (fast P velocity), $Z = \rho\alpha$ is the P-wave impedance, β is the vertical S-wave velocity ($S^{\|}$-wave, fast S velocity) $G = \rho\beta^2$ is the shear modulus, Δ denotes the difference in the elastic properties across the boundary. The average values of elastic properties in the two layer is denoted by the terms with overscores. $(\epsilon^{(V)}, \delta^{(V)}, \gamma)$ are the Thomsen-style

anisotropy parameters for HTI media. They are defined using stiffness coefficients as:

$$\begin{aligned} \epsilon^{(V)} &\equiv \frac{c_{11}-c_{33}}{2c_{33}}, \\ \delta^{(V)} &\equiv \frac{(c_{13}+c_{55})^2-(c_{33}-c_{55})^2}{2c_{33}(c_{33}-c_{55})}, \\ \gamma &\equiv \frac{c_{44}-c_{55}}{2c_{55}}. \end{aligned} \tag{2}$$

$\epsilon^{(V)}$ and γ describe the difference between vertical and horizontal wave velocities, and $\delta^{(V)}$ describes the departure from isotropy for near vertical propagation. This equation relates the AVO response to the anisotropy parameters and provides physical insight into the reflection amplitudes. Let's assume that the orientation ϕ_0 is known. Using Ruger's equation, we present a linear inversion to obtain the three anisotropy parameters.

We reformulate Rüger's equation as a function of P- and S-wave velocities using

$$\begin{aligned} \frac{\Delta Z}{\bar{Z}} &= \frac{\Delta\alpha}{\bar{\alpha}}+\frac{\Delta\rho}{\bar{\rho}}, \\ \frac{\Delta G}{\bar{G}} &= 2\frac{\Delta\beta}{\bar{\beta}}+\frac{\Delta\rho}{\bar{\rho}}. \end{aligned} \tag{3}$$

Equation 1 has the equivalent form

$$\begin{aligned} R_{PP}^{HTI}(\theta,\phi) \cong & \left(\frac{1}{2\cos^2\theta}\right)\frac{\Delta\alpha}{\bar{\alpha}} - \left(\frac{4\beta^2}{\alpha^2}\sin^2\theta\right)\frac{\Delta\beta}{\bar{\beta}} \\ & + \left(\frac{1}{2}-\frac{2\beta^2}{\alpha^2}\sin^2\theta\right)\frac{\Delta\rho}{\bar{\rho}} \\ & + \left(\frac{1}{2}\cos^4(\phi-\phi_0)\sin^2\theta\tan^2\theta\right)\Delta\epsilon^{(V)} \\ & + \left(\frac{1}{2}\cos^2(\phi-\phi_0)\sin^2\theta+\frac{1}{2}\cos^2(\phi-\phi_0)\sin^2(\phi-\phi_0)\sin^2\theta\tan^2\theta\right)\Delta\delta^{(V)} \\ & + \left(\frac{4\beta^2}{\alpha^2}\cos^2(\phi-\phi_0)\sin^2\theta\right)\Delta\gamma. \end{aligned} \tag{4}$$

The first three terms is the approximation given by Aki and Richards (1980) at a boundary between two isotropic media, The second three azimuthal dependent terms indicate the influence of each of the anisotropy parameters. Our AVAZ inversion for fracture intensity is based on equation 4.

Fracture orientation

Considering only small incident angle data (e.g., less than 35°), for which the $\sin^2\theta\tan^2\theta$ term can be neglected. Equation 1 can then be written as:

$$\left(G_1+G_2\cos^2(\phi-\phi_0)\right)\sin^2\theta, \tag{5}$$

where

$$I = \frac{1}{2}\frac{\Delta Z}{\bar{Z}}, \tag{6}$$

$$G_1 = \frac{1}{2}\left(\frac{\Delta\alpha}{\bar{\alpha}} - \left(\frac{2\bar{\beta}}{\bar{\alpha}}\right)^2 \frac{\Delta G}{\bar{G}}\right), \tag{7}$$

$$G_2 = \frac{1}{2}\left(\Delta\delta^{(V)} + 2\left(\frac{2\bar{\beta}}{\bar{\alpha}}\right)^2 \Delta\gamma\right). \tag{8}$$

Equation 5 describes the behavior of R_{PP}^{HTI} at small incident angles as a function of the AVO intercept and gradient. The gradient term

$$Q = G_1 + G_2\cos^2(\phi - \phi_0), \tag{9}$$

is composed of the azimuthally invariant term G_1, and an anisotropic term G_2, and is non-linear in the three unknowns $(G_1, G2, \phi 0)$. The goal here is to invert for the AVO gradient observed in amplitude data for these three unknowns. A description of a technique to bypass the non-linearity and to apply a linear inversion for these three unknowns follows.

Using the identity $\sin(\phi - \phi_0)^2 + \cos(\phi - \phi_0)^2 = 1$, the gradient term, equation 9 becomes

$$Q = (G_1 + G_2)\cos^2(\phi - \phi_0) + G_1\sin^2(\phi - \phi_0). \tag{10}$$

If the AVO gradient does not change sign azimuthally, the gradient versus azimuth vector delineates a curve that closely resembles an ellipse (Rüger, 2001) with the semi-axes aligned with the symmetry plane directions of the fracture system (Figure 1). With this in mind, let's perform a change of variable to align our coordinates with the fracture system. Let call the coordinate system aligned with the fracture system the (y_1, y_2), then every point of the gradient ellipse in this coordinate system has

$$\begin{aligned} y_1 &= r\cos(\phi - \phi_0), \\ y_2 &= r\sin(\phi - \phi_0), \end{aligned} \tag{11}$$

and r is the vector magnitude. In this coordinate system the gradient term can be written as:

$$Q = (G_1 + G_2)y_1^2 + G_1 y_2^2. \tag{12}$$

The acquisition coordinate system, $(x_1, x_2) = (r\cos\phi, r\sin\phi)$, can be thought of as a ϕ_0 rotated version of the (y_1, y_2) coordinate system (Figure 1). If we wish to write the gradient ellipse in equation 12 in the acquisition coordinate system, the ellipse equation inherits a nonlinear term x_1x_2, as in the form of

$$Q = W_{11}x_1^2 + 2W_{12}x_1x_2 + W_{22}x_2^2. \tag{13}$$

Equation 13 is a quadratic form, and can be written in a matrix form,

$$\begin{bmatrix} x_1 & x_2 \end{bmatrix} \begin{bmatrix} W_{11} & W_{12} \\ W_{12} & W_{22} \end{bmatrix} \begin{bmatrix} x_1 \\ x_2 \end{bmatrix} = X^T\mathbf{W}X. \tag{14}$$

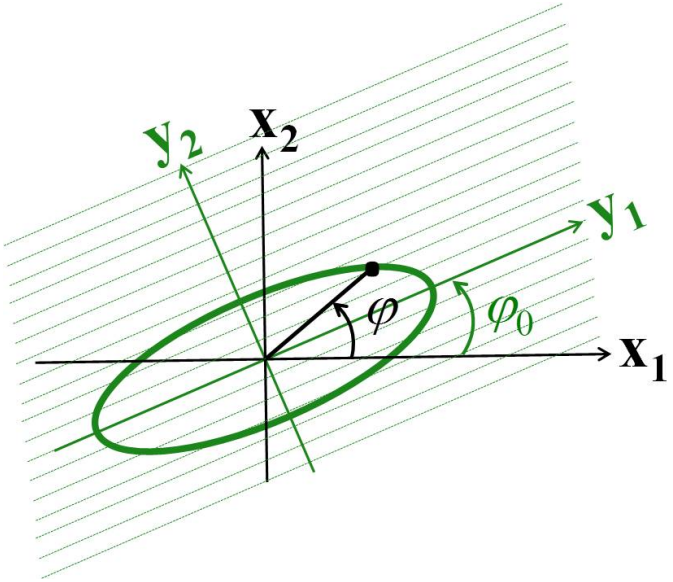

FIG. 1. Reference coordinate system. (x_1, x_2) is the acquisition coordinate system, and (y_1, y_2) is the coordinate system align with the fracture system. ϕ is the source-receiver azimuth, and ϕ_0 is the fracture orientation azimuth/

Using this form, the non-linearly with respect to the orientation is hidden in the W_{ij} coefficients. The matrix **W** is symmetric, and therefore orthogonality diagonalizable (e.g., Lax, 1997). By computing the eigenvalues,

$$\lambda_{1,2} = 0.5 \left[(W_{11} + W_{22}) \pm \sqrt{(W_{11} - W_{22})^2 + 4W_{12}^2} \right], \tag{15}$$

we can rewrite equation 13 in the form;

$$Q = \lambda_1 {y_1}^2 + \lambda_2 {y_2}^2. \tag{16}$$

Comparing coefficients from equations 16 and 12, we obtain: $G_1 + G_2 = \lambda_1$ and $G_1 = \lambda_2$, so:

$$\begin{aligned} G_1 &= 0.5 \left(W_{11} + W_{22} - \sqrt{(W_{11} - W_{22})^2 + 4W_{12}^2} \right), \\ G_2 &= \sqrt{(W_{11} - W_{22})^2 + 4W_{12}^2}. \end{aligned} \tag{17}$$

From the eigenvalue problem, we also know that orthogonal rotation matrix, R_{ϕ_0} relates the two coordinate system, as

$$\begin{bmatrix} y_1 \\ y_2 \end{bmatrix} = R_{\phi_0} \begin{bmatrix} x_1 \\ x_2 \end{bmatrix}, \tag{18}$$

where the rotation angle (ϕ_0) obeys (e.g., Lax, 1997)

$$\tan 2\phi_0 = \frac{2W_{12}}{W_{22} - W_{11}}. \tag{19}$$

This results in two values for ϕ_0 where $\phi_0^{(1)} = \pi/2 + \phi_0^{(2)}$. Using the trigonometric identity $\tan\phi_0 = \frac{2\tan\phi_0}{1-\tan{\phi_0}^2}$, we obtain two values for ϕ_0 as:

$$\phi_0^{(1)} = \tan^{-1}\left(\frac{W_{11} - W_{22} + \sqrt{(W_{11}-W_{22})^2 + 4W_{12}^2}}{2W_{12}}\right), \tag{20}$$

$$\phi_0^{(2)} = \tan^{-1}\left(\frac{W_{11} - W_{22} - \sqrt{(W_{11}-W_{22})^2 + 4W_{12}^2}}{2W_{12}}\right). \tag{21}$$

Equation 20 is used by Jenner (2002) without rigorous derivation, and is equivalent to what used by Grechka et al. (1999) in solving for fracture orientation form the azimuthal variation of NMO velocity.

AVAZ INVERSION FOR FRACTURE ORIENTATION

The approximation to the PP reflection coefficient using equation 5

$$R = I + \left(W_{11}\cos^2\phi + 2W_{12}\cos\phi\sin\phi + W_{22}\sin^2\phi\right), \tag{22}$$

where R is the pre-stack reflection amplitude, and ϕ is the acquisition source-receiver azimuth. Incorporating the amplitudes from different azimuths and small incident angles (e.g., up to 35°) as in the input data (R_{nm}), equation 22 can be used to express a linear system of "nm" equations in three unknowns:

$$\begin{bmatrix} \cos^2\phi_1\sin^2\theta_{11} & 2\cos\phi_1\sin\phi_1\sin^2\theta_{11} & \sin^2\phi_1\sin^2\theta_{11} \\ \vdots & \vdots & \vdots \\ \cos^2\phi_1\sin^2\theta_{n1} & 2\cos\phi_1\sin\phi_1\sin^2\theta_{n1} & \sin^2\phi_1\sin^2\theta_{n1} \\ \vdots & \vdots & \vdots \\ \vdots & \vdots & \vdots \\ \cos^2\phi_m\sin^2\theta_{1m} & 2\cos\phi_m\sin\phi_m\sin^2\theta_{1m} & \sin^2\phi_m\sin^2\theta_{1m} \\ \vdots & \vdots & \vdots \\ \cos^2\phi_m\sin^2\theta_{nm} & 2\cos\phi_m\sin\phi_m\sin^2\theta_{1m} & \sin^2\phi_m\sin^2\theta_{1m} \end{bmatrix}_{(nm\times 3)} \begin{bmatrix} W_{11} \\ W_{12} \\ W_{22} \end{bmatrix}_{(3\times 1)} = \begin{bmatrix} R_{11} - I \\ \vdots \\ R_{n1} - I \\ \vdots \\ \vdots \\ R_{1m} - I \\ \vdots \\ R_{nm} - I \end{bmatrix}_{(nm\times 1)} \tag{23}$$

where m is the number of azimuths, and n is the number of incident angles at each azimuth. The AVO intercept, I, is calculated using the vertical P-wave velocity and density. Equation 23 in matrix form can be written as,

$$G_{nm\times 3}X_{3\times 1} = R_{nm\times 1}. \tag{24}$$

The unknown vector $X = (W_{11}, W_{12}, W_{22})$ can be obtained from a damped least-squares inversion, as $X = (G^TG + \mu)^{-1}G^TR$ where μ is the damping factor. After the AVAZ inversion, knowing W_{ij}, we used equations 20 and 21 to estimate the fracture orientation.

AVAZ INVERSION FOR FRACTURE INTENSITY

Assuming the known fracture orientation, the PP reflection coefficient in equation 4 can be considered as a function of six parameters $(\frac{\Delta\alpha}{\bar{\alpha}}, \frac{\Delta\beta}{\bar{\beta}}, \frac{\Delta\rho}{\bar{\rho}}, \Delta\epsilon^{(V)}, \Delta\delta^{(V)}, \Delta\gamma)$. Equation 4

can be written as

$$R = A\frac{\Delta\alpha}{\bar{\alpha}} + B\frac{\Delta\beta}{\bar{\beta}} + C\frac{\Delta\rho}{\bar{\rho}} + D\,\Delta\epsilon^{(V)} + E\Delta\delta^{(V)} + F\Delta\gamma, \tag{25}$$

where R is the pre-stack reflection amplitude, and the coefficients A, B, C, D, E, and F are defined in of equation 4. These coefficients are functions of the incident angle, azimuth, and the background velocity model. Incorporating the amplitudes from different azimuths and incident angles (e.g., far-offset up to $45°$) as the input data in R_{mn} below, equation 25 can be used to express a linear system of "mn" equations in six unknowns:

$$\begin{bmatrix} A_{1\phi_1} & B_{1\phi_1} & C_{1\phi_1} & D_{1\phi_1} & E_{1\phi_1} & F_{1\phi_1} \\ \vdots & \vdots & \vdots & \vdots & \vdots & \vdots \\ A_{n\phi_1} & B_{n\phi_1} & C_{n\phi_1} & D_{n\phi_1} & E_{n\phi_1} & F_{n\phi_1} \\ \vdots & \vdots & \vdots & \vdots & \vdots & \vdots \\ \vdots & \vdots & \vdots & \vdots & \vdots & \vdots \\ A_{1\phi_m} & B_{1\phi_m} & C_{1\phi_m} & D_{1\phi_m} & E_{1\phi_m} & F_{1\phi_m} \\ \vdots & \vdots & \vdots & \vdots & \vdots & \vdots \\ A_{n\phi_m} & B_{n\phi_m} & C_{n\phi_m} & D_{n\phi_m} & E_{n\phi_m} & F_{n\phi_m} \end{bmatrix}_{(nm\times 6)} \begin{bmatrix} \Delta\alpha/\alpha \\ \Delta\beta/\beta \\ \Delta\rho/\rho \\ \Delta\delta \\ \Delta\varepsilon \\ \Delta\gamma \end{bmatrix}_{(6\times 1)} = \begin{bmatrix} R_{11} \\ \vdots \\ R_{n1} \\ \vdots \\ \vdots \\ R_{1m} \\ \vdots \\ R_{nm} \end{bmatrix}_{(nm\times 1)} \tag{26}$$

where m is the number of azimuths, and n is the number of incident angles at each azimuth. The coefficients are calculated using a smooth background isotropic velocity. Equation 26 in matrix form can be written as,

$$G_{nm\times 6}X_{6\times 1} = R_{nm\times 1}. \tag{27}$$

The unknown vector X can be obtained from a damped least-squares inversion, as $X = (G^TG + \mu)^{-1}G^TR$ where μ is the damping factor.

PHYSICAL MODEL REFLECTION DATA

We tested the proposed AVAZ inversions for fracture orientation and intensity on physical model reflection data acquired over a four-layered model, (Figure 2). Our model consists of isotropic water and plexiglas and an HTI layer composed of phenolic material. The construction of the experimental phenolic layer and its initial characterization are presented in another report (Mahmoudian et al., 2012a). The symmetry of phenolic materials is relatively well controlled. We found that the experimental phenolic layer approximates a weakly anisotropic HTI layer, or equivalently a vertically fractured transversely isotropic layer with known fracture orientation. The five independent parameters $(\alpha, \beta, \epsilon^{(V)}, \delta^{(V)}, \gamma)$ required to describe our simulated fractured medium are listed in Table 1.

Table 1. Elastic properties of the simulated fractured layer.

α (m/s)	β (m/s)	$\epsilon^{(V)}$	$\delta^{(V)}$	γ
3500	1700	-0.145	-0.185	0.117

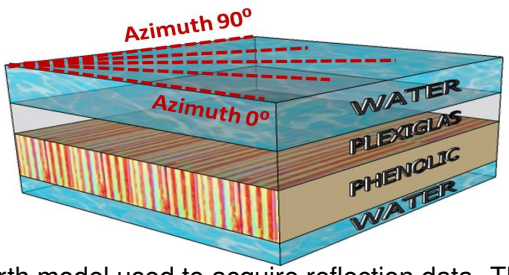

FIG. 2. The four-layered earth model used to acquire reflection data. The acquisition 0° azimuth is parallel to the fracture symmetry axis.

We used reflection amplitudes from nine long offset common midpoint (CMP) gathers acquired along 0°, 14°, 28°, 37°, 45°, 53°, 63°, 76°, and 90° azimuthal angles. Figure 3(a) shows the CMP seismic line acquired along the 90° azimuth (fracture plane). The amplitudes reflected from the top of the simulated fractured layer are inputs to AVAZ inversion. We manually picked the amplitudes and applied deterministic corrections to make them represent reflection coefficients required by an amplitude inversion. The corrections for geometrical spreading, emergence angle, transmission loss, and source-receiver transducer directivity have been applied. A detailed description for the data acquisition and corrections is given in another report (Mahmoudian et al., 2012b).

The corrected reflected amplitudes from the top of the fractured layer for nine azimuths between 0° and 90° are shown in Figure 4. The large oscillations in the amplitude data are due to the interference with the top reflector reverberations which has a different dip than the target event, Figure 3(b) shows the wave interference effect on the target amplitudes. The presence of large oscillations in the data causes the AVAZ inversion to be unstable depending on the maximum incident angle used. To avoid unstable inversion, we smooth the amplitude data prior to inversion. Smoothing is applied by using the best fit polynomial of degree $n = 10$ to the amplitude data. The smoothed amplitude data are shown in Figure 5.

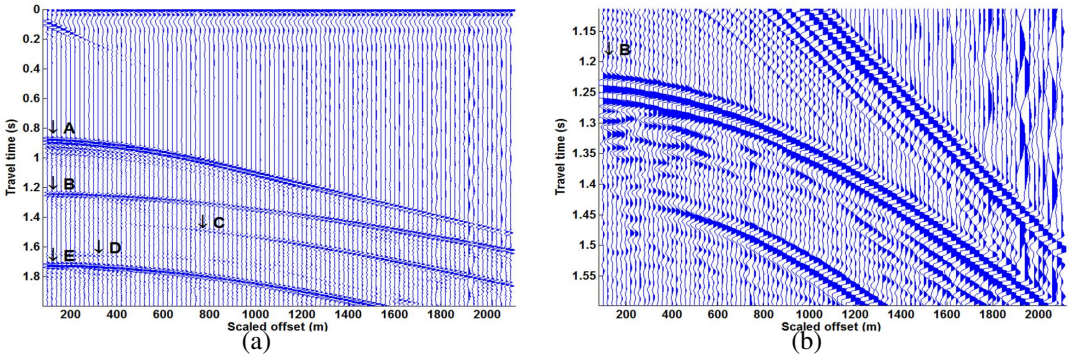

FIG. 3. (a) 90° azimuth data with a long gate automatic gain control applied. In the display,event "A" is the PP reflection from the top of the plexiglas layer, event "B" is the PP reflection from the top of the fractured layer (our target), event "C" is the PS reflection from the top of the fractured layer, event "D" is the PP reflection from the bottom of the fractured layer, and event "E" is the PP reflection from the base layer. (b) 90° azimuth data, zoomed on the target reflector, note the top reflector reverberations' interference with the target event.

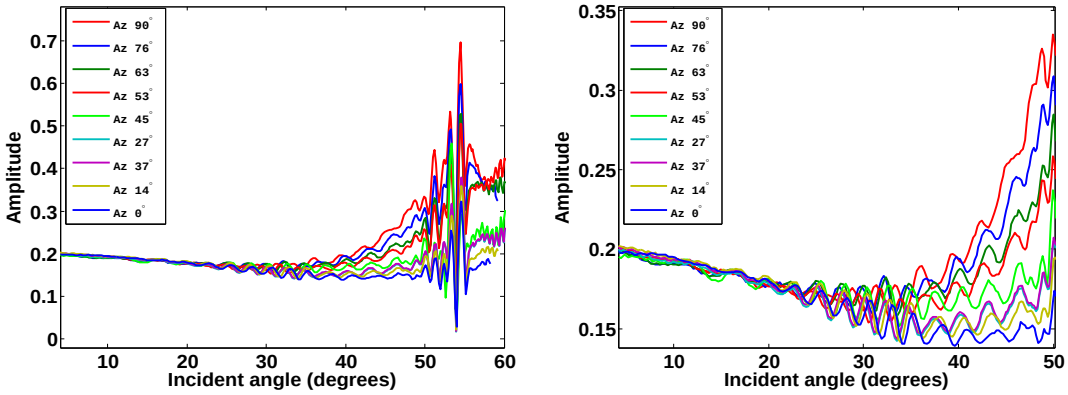

FIG. 4. Fracture top corrected reflection amplitudes from all nine azimuths. (a) All incident angles,(b) the incident angles before the critical angle.

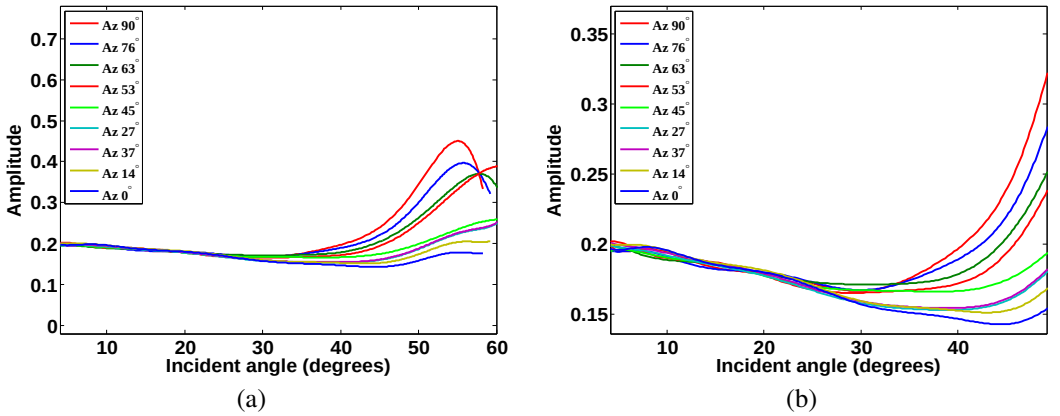

FIG. 5. Fracture top smooth amplitude data input to the AVAZ inversions. (a) All incident angles,(b) the incident angles before the critical angle.

ESTIMATED ORIENTATION OF THE SIMULATED FRACTURED LAYER

We use small incident angle data (maximum incident angle of $35°$) in the AVAZ inversion based on equation 23 for the fracture orientation. Since the symmetry of the simulated fractured medium is known and the physical model data acquisition coordinate was aligned with the fracture system, we rotate our acquisition coordinate system to arbitrary directions and used the proposed AVAZ inversion to estimate the fracture orientation. Table 2 shows the predicted fracture orientations.

Table 2. Estimated fracture orientation from the AVAZ inversion.

True ϕ_0	-0	20	40	50	60	80	90
Estimated ϕ_0	-1.5	18.5	38.5	48.5	5 8.5	78.5	88.5
	88.5	108.5	128.5	138.5	148.5	168.5	178.5

The method is successful in predicting the fracture orientation; however, there is an ambiguity in the estimation as the method predicts both the fracture orientation and the direction normal (symmetry axis) to it. Therefore, a priori knowledge of the fracture orientation is required, perhaps from NMO analysis.

ESTIMATED ANISOTROPY PARAMETERS OF THE SIMULATED FRACTURED MEDIUM

Knowing the fracture orientation for our simulated fractured medium, we test the proposed six-parameter AVAZ inversion on the physical model data. In the first implementation, we estimate all six parameters $(\Delta\alpha/\alpha, \Delta\beta/\beta, \Delta\rho/\rho, \epsilon^{(V)}, \epsilon^{(V)}, \gamma)$ simultaneously, using equation 26. For a given offset and depth of the fractured layer, the primary ray-path is traced to determine the incident angle, using a PP raytracing code. Then the coefficient matrix (coefficients are function of the incident angle and background velocity model) in equation 26 are calculated.

The azimuthal variation of our amplitude data before 30° is very small (Figure 4), and incorporating larger incident angles are required. Figure 6 shows the six-parameter AVAZ inversion for different maximum incorporated incident angles, indicating that for the right choice of the maximum incorporated incident angle, the linear AVAZ inversion results in reasonable estimates for all six parameters. The critical angle for plexiglas/phenolic is around 50°. The six-parameter AVAZ inversion results demonstrated in Figure 6 indicate the following points:

1. the six-parameter AVAZ inversion using small incident angles, less than 35°, does not produce good estimates for any of the six parameters, as there are not enough data in the inversion.
2. Incorporating large incident angles (e.g., 40°) up to 10° before the critical angle can result in reasonable estimates for all the six parameters. The isotropic terms $(\Delta\alpha/\alpha, \Delta\beta/\beta, \Delta\rho/\rho)$, however, are estimated with much smaller errors compared to the anisotropic terms, indicating of the larger influence of the isotopic terms on the reflection coefficients.
3. Incorporating very large incident angles, closer to the critical angle, results in better estimates for the anisotropy parameters as the azimuthal anisotropy is more pronounced at larger incident angle data. However, it produces large errors for the estimates of the three isotropic terms. The anisotropy parameters $\epsilon^{(V)}$ and γ are more accurately estimated, but the $\delta^{(V)}$ parameter which governs the near-vertical wave propagation losses its accuracy. The overall error for all six parameters are larger when incorporating incident angles close to the critical angle, as the linear Rüger's equation not valid in this region.

In an effort to obtain better estimates for the anisotropic terms, we used a second implementation in which we applied some constraints to the three isotropic terms. There are many other methods available to estimate the vertical P- and S-wave velocity and density such as the AVA inversion of single azimuth data or by incorporating well log information. We put three different constraints on these first three variables using the estimated values of α, β and ρ from an AVA inversion of 90° (isotropic plane) azimuth data. Figure 7 shows these constraints. With such constraints, the inversion results for the three anisotropy parameters, for various maximum incorporated incident angles, are shown in Figure 8. As a result of these constraints, for the right choose of the maximum incorporated incident

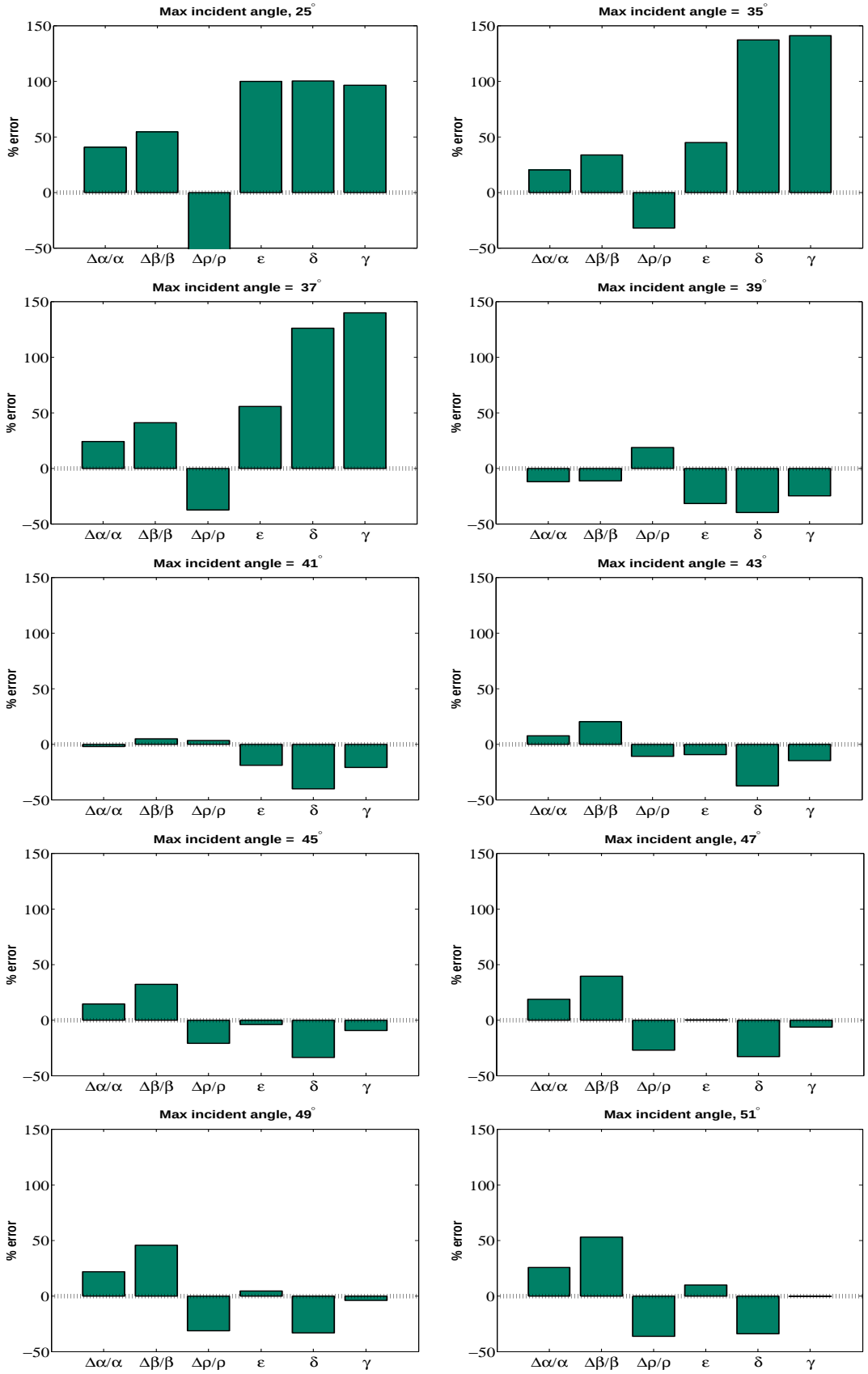

FIG. 6. Six-parameter AVAZ inversion for various maximum incorporated incident angles. The estimate are compared to the values previously estimated from traveltime inversion.

angle, the inversion results for $\epsilon^{(V)}$, $\delta^{(V)}$, and γ agree very favorably with those obtained previously by traveltime inversion. For the right choice of the maximum incorporated incident angle, the estimate for anisotropy parameters from constrained AVAZ inversion is within 10%; these estimates are better compared to the estimates of the simultaneous six-parameter inversion (Figure 6).

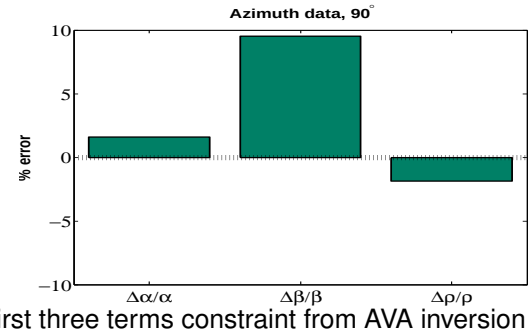

FIG. 7. First three terms constraint from AVA inversion of 90° data.

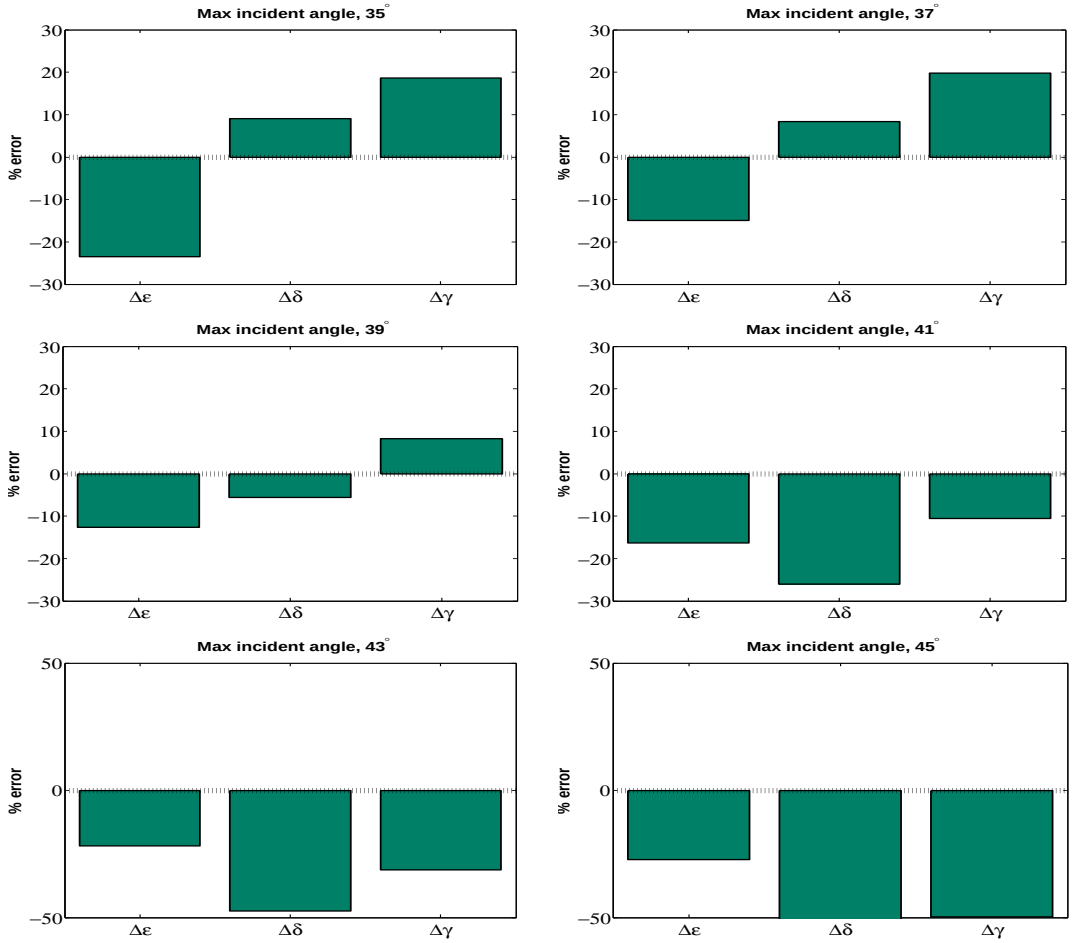

FIG. 8. Constrained AVAZ inversion for anisotropy parameters.

CONCLUSIONS

We presented pre-stack amplitude inversion procedures to extract the anisotropy parameters $(\epsilon^{(V)}, \delta^{(V)}, \gamma)$, and fracture orientation from the azimuthal variations in the PP reflection amplitudes. As the shear-wave splitting factor, γ parameter, is directly related to fracture intensity, we showed that it is possible to relate the difference in P-wave azimuthal AVO variations directly to the fracture intensity of our simulated fracture layer. Accurate linear inversion for the anisotropy parameters requires the employing of large-offset data. However, incorporating very large offset data close to the critical angle should be avoided as the linear Rüger's equation is a plane wave solution and not valid close to the critical angle.

The AVAZ inversion determines the fracture orientation with an inherent ambiguity, as it predicts both the directions of the isotropic plane and symmetry axis of an HTI medium. For an accurate prediction of the fracture orientation some other information is required, such as azimuthal NMO and shear-wave splitting. These effects are qualitatively different from azimuthal AVO and can be combined effectively to invert for fracture orientation.

Our inversion is based on the approximate reflection coefficients by Rüger (2001). Our inversion estimates demonstrate that the Rüger's equation is suitable for quantitative amplitude analysis of anisotropic targets, and can be employed for numerical inversion algorithms.

ACKNOWLEDGEMENTS

We thank the sponsors of CREWES for their financial support. We are grateful to Dr. Joe Wong for acquiring the physical modeling data. Dr. P.F. Daley, Dr. Kris Innanen, Mahdi Al-Mutlaq, and Marcus Wilson are acknowledged for their suggestions.

REFERENCES

Aki, K., and Richards, P. G., 1980, Quantitative Seismology: W. H. Freeman and Company, San Francisco.

Crampin, S., 1981, A review of wave motion in anisotropic and cracked elastic media: Wave Motion, **3**, 343–391.

Grechka, V., Theophanis, S., and Tsvankin, I., 1999, Joint inversion of p- and ps- waves in orthorhombic media: Theory and a physical modeling study, **64**.

Jenner, E., 2002, Azimuthal avo: methodology and data example: The Leading Edge, **21**, No. 8, 782–786.

Lax, P. D., 1997, Linear algebra and its applications:

Mahmoudian, F., Margrave, G. F., Daley, P. F., and Wong, J., 2012a, Estimation of stiffness coefficients of an orthorhombic physical model from group velocity measurements: CREWES Reports.

Mahmoudian, F., Margrave, G. F., and Wong, J., 2012b, Azimuthal avo over a simulated fractured physical model medium: CREWES Reports.

Nelson, R. A., 2001, Geologic analysis of naturally fractured reservoirs, Second edition: Elsevier.

Rüger, A., 2001, Reflection coefficients and azimuthal AVO analysis in anisotropic media: Goephysical Monograph Series.

Thomson, L., 1986, Weak elastic anisotropy: Geophysics, **51**, 1954–1966.

Tsvankin, I., 2001, Seismic signatures and analysis of reflection coefficients in anisotropic media: Elsevier, Amsterdam.

Zheng, Y., 2006, Seismic azimuthal anisotropy and fracture analysis from pp reflection data: PhD. Thesis, University of Calgary.

Zheng, Y., and Wang, S., 2005, Fracture analysis on prestack migrated gathers: A physical modeling study: CSEG Expanded Abstracts.